Doklady Earth Sciences, Vol. 397A, No. 6, 2004, pp. 816–819. Translated from Doklady Akademii Nauk, Vol. 397, No. 3, 2004, pp. 404–407.

GEOPHYSICS

Fine Structure of Beams of a Three-Dimensional Periodic Internal Wave

Yu. D. Chashechkin, A. Yu. Vasil'ev, and R. N. Bardakov

Presented by Academician G.S. Golitsyn March 11, 2004

Received March 12, 2004

Internal waves in oceans, the atmosphere, and laboratories are often observed as compact groups consisting of few spatial oscillations [1–3]. In a laboratory environment, the spatial structure of inner wave beams is characterized by a scale depending on the source size, buoyancy frequency, kinematic viscosity, and distance to the observation point [4, 5]. However, when smooth beams cross a column of continuously stratified fluid, the oscillation amplitude increase caused by nonlinear interaction of waves [6] is supplemented with the formation of thin high-gradient sublayers [7, 8]. Extended discontinuities of the smooth profile of the buoyancy frequency have a sufficiently regular form. Near-horizontal sublayers are also observed during the collision of internal solitons [9].

The sublayers are always confined to the beam intersections zone, and their thickness is essentially smaller than the length of the interacting waves. The mechanism of "stratification fault" [7] formation governing the transfer of impulse, mass, and the energy is still unknown. Study of this mechanism is of interest to identify processes of the formation of the universally observed fine structure of oceans and atmosphere [10, 11], as well as to analyze the role of dissipation factors in the mechanics of periodic movements of fluids.

This work studies the fine structure of beams of three-dimensional (3D) periodic internal waves (PIW) using analytical and numerical methods. Taking into consideration the symmetry of internal waves, the source chosen is a disk of radius R that lies on a solid horizontal surface and vertically oscillates with frequency ω and small velocity amplitude U.

The linearized equation system for the movement of exponentially stratified viscous fluid in the Boussinesq approximation has the form [12]

$$\frac{\partial v_r}{\partial t} = -\frac{1}{\rho_0}\frac{\partial P}{\partial r} + \nu\left(\Delta v_r - \frac{v_r}{r^2}\right),$$

$$\frac{\partial v_z}{\partial t} = -\frac{1}{\rho_0}\frac{\partial P}{\partial z} + \nu\Delta v_z - g, \qquad (1)$$

$$\frac{\partial \rho}{\partial t} + v_z\frac{\partial \rho_0}{\partial z} = 0, \quad \frac{\partial v_r}{\partial r} + \frac{v_r}{r} + \frac{\partial v_z}{\partial z} = 0,$$

where $\mathbf{v}$ is the velocity; P and ρ are the perturbations of pressure and density, respectively; $\rho_0(z) = \rho_{00}\exp\left(-\frac{z}{\Lambda}\right)$ is the initial density distribution; Λ is the buoyancy scale; ν is the kinematic viscosity; g is the gravity acceleration; $\Delta = \frac{\partial^2}{\partial r^2} + \frac{1}{r}\frac{\partial}{\partial r} + \frac{\partial^2}{\partial z^2}$; and the z axis of a cylindrical reference system (r, φ, z) is directed upward against the gravity force. The diffusion and thermal conductivity effects are neglected.

The adhesion boundary conditions are set both at the oscillating disc and at the remaining part of the horizontal plane

$$v_r\big|_{z=0} = 0,$$

$$v_z\big|_{z=0} = \begin{cases} U, & r \le R \\ 0, & r > R. \end{cases} \qquad (2)$$

At infinity ($z \to \infty$) all the perturbations fade out. The steady state motions are considered when all the functions harmonically change with time as $\exp(-i\omega t)$. This factor is omitted for brevity.

Taking into consideration incompressibility and axial symmetry, system (1) is transformed into an equation for the scalar function, Ψ, that defines the components of velocity $\mathbf{v}$ in the cylindrical reference system connected with the disc center as

$$v_r = \frac{\partial \Psi}{\partial z}, \quad v_z = -\frac{\partial \Psi}{\partial r} - \frac{\Psi}{r}. \qquad (3)$$

Institute for Problems of Mechanics,
Russian Academy of Science, pr. Vernadskogo 101, Moscow, 117526 Russia; e-mail: chakin@ipmnet.ru

Then, system (1) and boundary conditions (2) take the following form:

$$\left[-\omega^2\left(\Delta-\frac{1}{r^2}\right)+N^2\left(\Delta_\perp-\frac{1}{r^2}\right)+i\nu\omega\left(\Delta-\frac{1}{r^2}\right)^2\right]\Psi=0, \quad (4)$$

$$\left.\frac{\partial\Psi}{\partial z}\right|_{z=0}=0, \quad \left.\left(\frac{\partial\Psi}{\partial r}+\frac{\Psi}{r}\right)\right|_{z=0}=-U\vartheta(R-r), \quad (5)$$

where $\Delta_\perp=\Delta-\frac{\partial^2}{\partial z^2}$, $N=\sqrt{\frac{g}{\Lambda}}$ is the buoyancy frequency, and ϑ is the Heaviside function.

Generally, a double boundary layer consisting of inner and isopycnal (Stokes) sublayers is formed at the surface emitting internal waves. The parameters of the sublayers depend on the medium properties, wave frequency, and geometry of the problem [5]. At the source considered, where the axial component of the fluid velocity vanishes, the inner boundary layer transforms to the Stokes one and the isopycnal one disappears. In this case, the number of roots of the dispersion equation is less than in the common case [5] and the solution of (4) under the boundary conditions (5),

$$\Psi=UR\int_0^\infty\frac{J_1(kr)J_1(kr)}{k(k_2-k_1)}[k_2e^{ik_1(k)z}+k_1e^{ik_2(k)z}]dk \quad (6)$$

only includes the following regular (proportional to ν) and singular $\left(\sim\frac{1}{\sqrt{\nu}}\right)$ roots of the dispersion equation:

$$\omega^2(k^2+k_{1,2}^2)-N^2k^2+i\nu\omega(k^2+k_{1,2}^2)^2=0:$$

$$k_1^2=-k^2+\frac{i\sin\theta}{2\delta_N^2}\left[1-\sqrt{1+\frac{4ik^2\delta_N^2}{\sin^3\theta}}\right],$$
$$k_2^2=-k^2+\frac{i\sin\theta}{2\delta_N^2}\left[1+\sqrt{1+\frac{4ik^2\delta_N^2}{\sin^3\theta}}\right]. \quad (7)$$

Here, $\delta_N=\sqrt{\frac{\nu}{N}}$ is the universal microscale of periodic perturbations and $\theta=\arcsin\frac{\omega}{N}$ is the wave cone inclination to the horizon.

To satisfy the damping conditions at infinity in the upper half plane ($z\geq 0$), the following roots should be chosen: $\mathrm{Im}\,k_1>0$ and $\mathrm{Im}\,k_2>0$. The spatial structure of the wave cone is defined by the imaginary part of solution (6), which is not small even if the stratification is weak and the viscosity is small.

The asymptotic expressions for the roots (7) are

$$k_1=-|k|\cot\theta+\frac{i\delta_N|k|^3}{2\cos\theta\sin^4\theta}, \quad k_2=\frac{i+1}{\delta_N}\sqrt{\frac{\sin\theta}{2}}.$$

The wave number k_1 relates to the traveling internal waves, while k_2 relates to the boundary layer with typical thickness $\delta_\omega=\delta_N\sqrt{\frac{\sin\theta}{2}}$.

From (6) follow the expressions for the vertical and radial velocities,

$$v_z=UR\int_0^\infty\frac{J_1(kR)J_0(kr)}{k_2-k_1}(k_2e^{ik_1z}-k_1e^{ik_2z})dk, \quad (8)$$

$$v_r=-iUR\int_0^\infty\frac{k_2k_1}{k_2-k_1}\frac{J_1(kR)J_1(kr)}{k}(e^{ik_1z}-e^{ik_2z})dk \quad (9)$$

and for the vorticity components,

$$\Omega_\alpha=UR\int_0^\infty\frac{dk}{k_2-k_1}\frac{J_1(kr)J_1(kR)}{k}$$
$$\times(k_2e^{ik_1z}-k_1e^{ik_2z})(k_1k_2-k^2). \quad (10)$$

Far from the disc ($r\gg R$) with a smaller radius (relative to the viscosity wave scale $R\ll L_\nu$, $L_\nu=\left(\frac{\nu\Lambda}{N}\right)^{1/3}$) in the concomitant reference system (q, p) and the axes oriented along the cone generator and along the normal to wave cone, the asymptotic expression for the vertical velocity takes the canonical form [4]

$$v_z(p,q)=\frac{1-i}{\sqrt{\pi}}UR^2\sin\theta\sqrt{\frac{\sin\theta}{p\sin\theta+q\cos\theta}}$$
$$\times\int_0^\infty k_p^{1/2}\exp\left(ik_pp-\frac{\nu k_p^3q}{2N\cos\theta}\right)dk_p. \quad (11)$$

As follows from (11), the amplitude of 3D periodic waves falls inversely with distance from the source, the oscillations across the beam rapidly fading. Asymptotic expression (11) only describes the regular velocity component. It is more convenient to calculate the boundary layers using the boundary function method.

In the low-viscosity approximation, the items in the expression for the vertical component of the force acting upon the vibrating disk surface,

$$F_z|_{z=0}=(1+i)\rho_0UR^2\left(-\frac{8\omega R\cot\theta}{3}+\frac{\pi^2\sqrt{\omega\nu}}{\sqrt{2}}\right) \quad (12)$$

differ from the inertial and dissipative components of the resistance force acting upon a sphere oscillating in

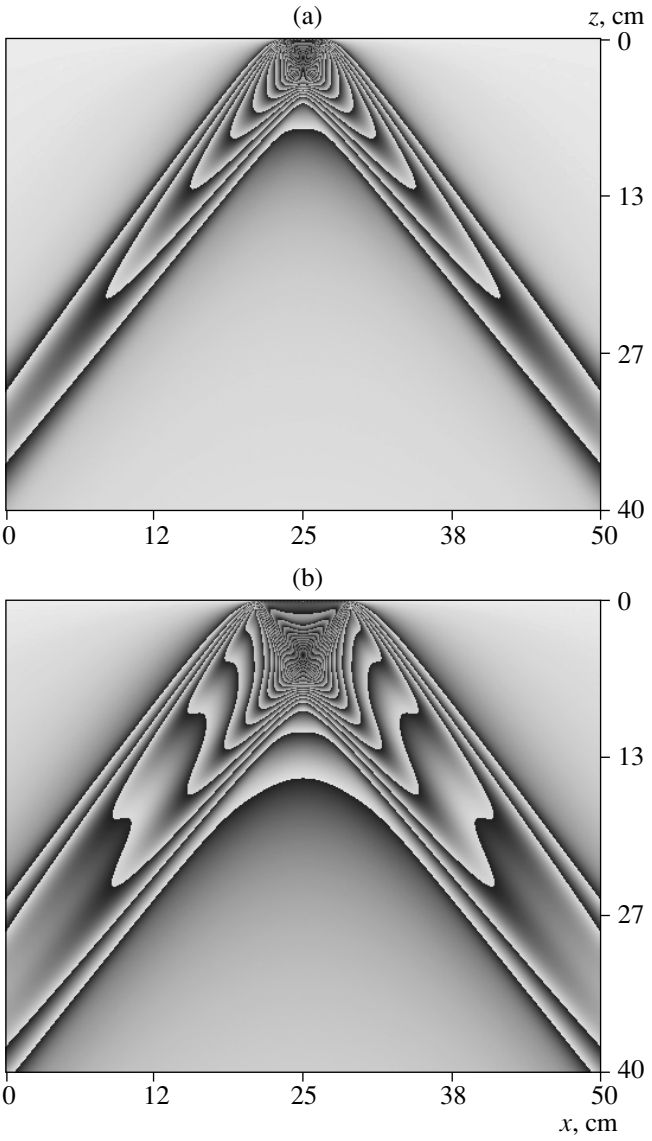

Fig. 1. Mode structure of periodic wave cone beams generated by horizontal (a) small (R = 1.7 cm) and (b) large (R = 4 cm) discs. Vertical velocity distribution in the central section of the beam is shown. N = 1.2 s^{-1}; ω = 0.998 s^{-1}, U = 0.25 cm/s, t = 0.

homogeneous fluid [12] by factors $4(1 + i)\frac{\cot\theta}{\pi}$ and $\frac{\pi(1+i)}{6}$, respectively. Both the exact solution (6) and the asymptotic representation (11) include only the problem parameters, in contrast to [3], where it is necessary to empirically define the properties of the model sources and sinks. The fine structure of the wave beams described by exact solution (6) is further studied by numerical methods.

In order to reproduce the flow structure, array values (8) and (9) are computed using the Simpson method at the grid points, with parameters chosen so as to visualize the flow elements with resolution of 0.1–0.02 mm. The upper limits of integration intervals are chosen so as to preserve calculation accuracy within the whole range of the problem parameters. The full-color visualization program code is written in MS Visual C++. Only black-and-white images are presented here. The computation shows that it is possible to visualize both the boundary layer at the emitting surface and the wave fields in the entire space.

The mode structure of PIW conic beams generated by different-sized discs is shown in Fig. 1 (the buoyancy frequency, as well as the frequency and amplitude of vertical oscillations of the source, are constant in either case). The flow image is based on the modified method of isolines $\left(25 \text{ lines, with a pitch of } \frac{U}{26}\right)$. The small disc ($R$ = 1.7 cm, $R < L_v$) emits a single-mode beam with the displacement maximum at the center (Fig. 1a). The distribution of the vertical velocity module in the internal wave beam emitted by the wide disk (R = 4 cm, $R > L_v$; Fig. 1b) shows two maximums at the beam edges.

The distributions of the velocity module and vertical component across the beam also remain symmetrical in the latter case [2, 4]. Boundary layers at the plane extend beyond the source and their perturbation phases are coherent with the wave ones. Extended inhomogeneities are located at the outer boundaries of the beams. Since the cross size is small, the fine structure rapidly and synchronically evolves in the whole observation area.

The fine structure of perturbations becomes more prominent when we utilize "differential analyzers" acting as schlieren instruments used in experimental hydrodynamics. The image of the first derivative of the vertical velocity, also based on the modified method of isolines (Fig. 2a), is sufficiently contrasting to demonstrate the fine structure of the wave beam shells with cross section size of approximately δ_N generated by the disc edge. The total number of isolines is 50. The pitch is equal to $\frac{1}{51}$ of the first derivative maximum (2.41 s^{-1}) at the intersection of the inner beam shells. Two perturbation bands forming the inner and outer shells of the beam cone are generated by the disc edge. Their contrast ratios and cross section sizes change with time much more rapidly than the entire wave image. The fine beam shells are even more contrasting in the image of the second derivative of the velocity (50 isolines with pitch equal to 1/51 of the velocity second derivative module maximum (22.7 cm^{-1} s^{-1}) at the disc edges). At the beam periphery, the velocity shift decreases with distance sufficiently slowly.

The superposition and nonlinear enhancement of gradients at the intersection of the structure elements—δ_N thick—may lead to the origination of stratification

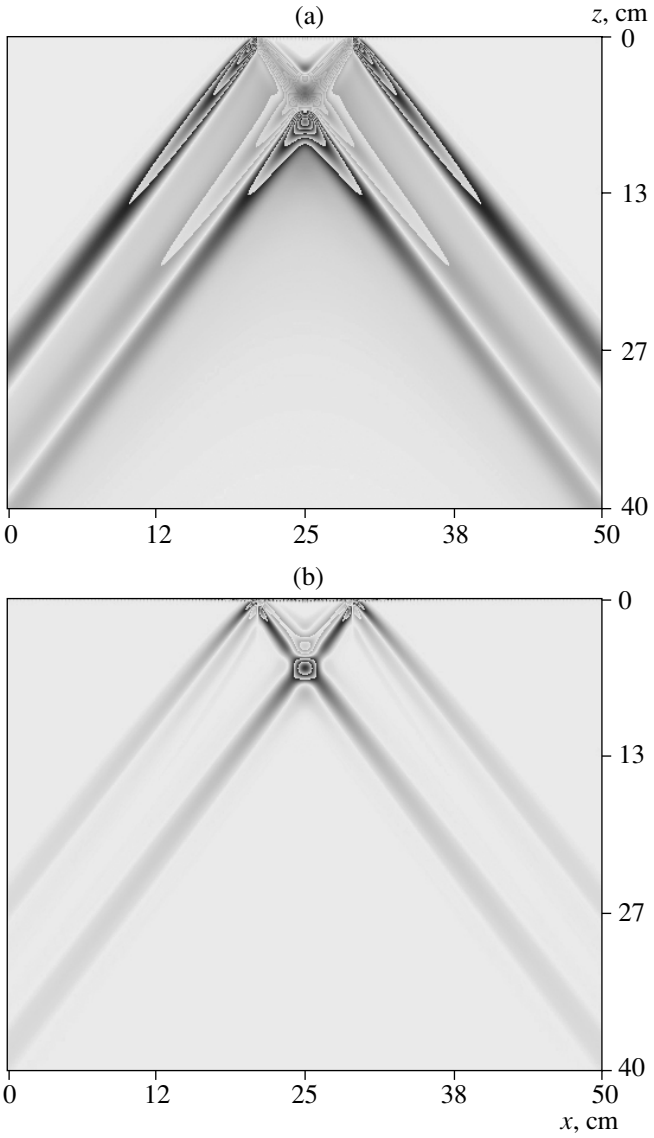

Fig. 2. Fine structure shells of two-mode beams of 3D periodic internal waves. Distributions of the (a) first $\frac{\partial v_r}{\partial z}$ and (b) second $\frac{\partial^2 v_r}{\partial z^2}$ derivatives of the radial velocity in the central section of the conic beam. $N = 1.2\ s^{-1}$; $\omega = 1.0\ s^{-1}$; $R = 4$ cm; $L_v = 1.8$ cm; $U = 0.25$ cm/s; $t = 0$.

discontinuities [6–8]. In order to confidently record and measure singular element parameters relative to large-scale internal waves, it is necessary use fast gages with resolution of δ_N, which is only accessible for the best schlieren instruments.

ACKNOWLEDGMENTS

This work was supported by the Russian Academy of Science (Program "Dynamics and Acoustics of Inhomogeneous Fluids, Gas–Fluid Mixtures, and Slips"), the "Integratsiya" federal program of the Russian Ministry of Education (project no. 02-Ya0058/993), and the Russian Foundation for Basic Research (project no. 02-05-65383).

REFERENCES

1. C. P. Summerhayes and S. A. Thorpe, *Oceanography. An Illustrated Guide* (Manson Publ., Mexico, 1996).
2. V. N. Kozhevnikov, *Atmospheric Perturbations during Flow Around Hills* (Nauchny Mir, Moscow, 1999) [in Russian].
3. J. Lighthill, *Waves in Fluids* (Mir, Moscow, 1981) [in Russian].
4. Yu. V. Kistovich and Yu. D. Chashechkin, J. Appl. Mech. Tech. Phys. **42**, 52 (2001).
5. A. Yu. Vasil'ev and Yu. D. Chashechkin, J Appl. Math and Mech. **67**, 442 (2003).
6. Yu. D. Chashechkin and V. I. Nekludov, Dokl. Akad. Nauk SSSR **311**, 970 (1990).
7. A. D. McEwan and P. A. Plumb, Dyn. Atmos. and Oceans **2**, 83 (1977).
8. S. G. Teoh, G. N. Ivey, and J. J. Imberger, Fluid. Mech., **336**, 91 (1997).
9. H. Honji, N. Matsunaga, Y. Sugihara, and K. Sakai, Fluid Dyn. Res. **15**, 89 (1995).
10. K. N. Fedorov, *Fine Thermohaline Structure of Ocean Waters* (Gidrometeoizdat, Leningrad, 1976) [in Russian].
11. F. Dalaudier, C. Sidi, M. Crochet, J. Vernin, J. Atmos. Sci. **51**, 237 (1994).
12. L. D. Landau and E. M. Lifshits, *Hydrodinamics* (Nauka, Moscow, 2000) [in Russian].